Impact of the 2011 tsunami on the littoral system around offshore breakwaters on Sendai Coast

H. Tanaka & Y. Mitobe
Tohoku University, Sendai, Japan

A. Mori
Tokyo Electric Power Company, Tokyo, Japan

ABSTRACT: After the 2011 Great East Japan Earthquake Tsunami, littoral system on Sendai Coast have been changing due to tsunami-induced highly non-equilibrium condition along the coast. In order to clarify the modification of littoral environment and its subsequent recovery on Sendai Coast, analysis of shoreline change has been carried out. In this study, the shoreline was extracted from frequently captured aerial photographs from 2009 until now, and analysis using an empirical orthogonal function (EOF) method was conducted. It is seen that the shoreline retreated greatly due to tsunami event. In particular, tombolo which existed behind the offshore breakwater completely disappeared due to the tsunami. Total of contribution of the 1st and 2nd EOF components is more than 70%. It is concluded that the 1st component originated from cross-shore sediment movement, while the 2nd component represents longshore sediment transport. Although the 1st component shows only slight modification after the tsunami, the 2nd component resulting from a longshore sediment transport shows distinct change after the tsunami around the offshore breakwaters.

1 INTRODUCTION

The Great East Japan Earthquake which occurred on March 11, 2011 caused serious damages in Tohoku District in Japan. In addition it caused extreme geographical changes in localized areas such as river mouths and location of old rivers (Tanaka et al., 2012, Udo et al., 2012). Sandy coast around offshore breakwaters is also area in which serious erosion occurred due to the 2011 Tsunami. This localized morphology change resulted in highly non-equilibrium littoral system along the sandy coast.

In the present study, pre- and post-tsunami morphology change around offshore breakwaters on Sendai Coast, Japan is investigated. The offshore breakwaters on Sendai Coast have been constructed from 1970s to 1980s by the prefectural government, and its effectiveness of the structure has already been investigated and confirmed by Numata and Takahashi (1983) by analyzing bathymetry data as well as aerial photographs in this region. Kang and Tanaka (2005) used long-term aerial photographs in this area to evaluate longshore distribution of longshore sediment transport rate. They concluded that the offshore breakwaters are affecting not only to cross-shore sediment movement, but also to longshore sediment movement along the coast.

Because the morphological change induced by the 2011 Great East Japan Earthquake Tsunami was highly localized as mentioned above, littoral environment along the coast has been modified as compared with the pre-tsunami situation. Therefore, this study investigates the geographical recovery process around the offshore breakwaters after tsunami occurrence based on analysis of highly frequent aerial photographs captured almost every two months.

2 STUDY AREA AND METHODOLOGY

2.1 *Sendai Coast*

In this study, behavior of sandy coast about 4.5km long around offshore breakwaters on Sendai Coasts, Miyagi Prefecture, Japan is investigated. The location of the study area is depicted in Figure 1. Construction of the offshore breakwaters on this coast started in 1976 in order to prevent further beach erosion, and in total six offshore breakwaters have been constructed by the prefectural government. After completion of the construction, sediment has accumulated behind the offshore breakwater, resulting in formation of tombolo as seen in Figure 1.

The predominant direction of longshore sediment transport on Sendai Coast is from south to north due to incident waves from southeast to east-southeast directions (Kang and Tanaka, 2005), causing sediment deposit in the updrift area of the offshore breakwater, and vice versa.
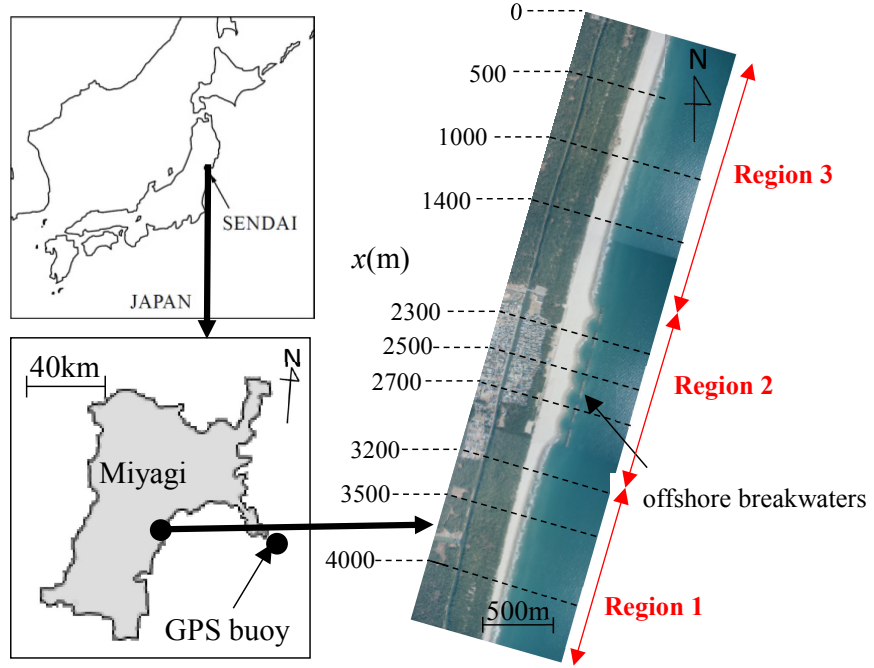
Figure 1. Study area

2.2 *Methodology*

In this study, aerial photographs captured every one or two months covering both pre- and post-tsunami periods (from March, 2009 to January, 2015) has been used. Considering capturing time of aerial photograph, influence of tidal elevation and wave run-up height were removed to define the shoreline position with respect to the mean sea level. In order estimate wave run-up height from wave condition, Eq.(1) proposed by Hunt (1959) has been used.

$$\frac{R}{H_0} = \xi_0 \qquad (1)$$

where R is the wave run-up height, H_0 is the deep water wave height, and ξ_0: the surf similarity parameter.

3 RESULTS AND DISCUSSION

3.1 *Shoreline change*

Temporal variation of shoreline position is depicted in Figure 2 for three regions defined in Figure 1; Region 1, Region 2 and Region 3 from the south to the north.

In Region 1 located in the southern updrift area, influence of the tsunami is not clearly observed in the shoreline change as seen in Figure 2(a). Gradual retreat of the shoreline can be observed during whole of the period covering both pre- and post-tsunami periods.

In Region 2 located behind the offshore breakwaters in Figure 2(b), sudden retreat of shoreline occurred due to the tsunami on March 11, 2011. Subsequently shoreline shows gradual advancement, corresponding to regrowth of tombolo behind the offshore breakwaters. It seems the shoreline position in this region already reached equilibrium in 2014, although it is showing fluctuations in response to wave condition.

In Region 3 illustrated in Figure 2(c), sudden retreat of shoreline can be seen immediately after the tsunami occurrence, and gradual retreat is still ongoing even now. It is noted that the shoreline response in the three regions are highly different each other as described here.

In order to evaluate shoreline behavior more quantitatively, regression analysis is applied for each location along the coast. Thus shoreline variation is expressed by the following linear equation separately for pre- and post-tsunami periods.

$$y_s = at + b \qquad (2)$$

where a, b are the coefficients and t is the time.

The rate of shoreline change, a, is plotted in Figure 3 for the period pre- and post-tsunami. Before the tsunami attack, both Region 1 and Region 2 show shoreline advancement due to the offshore breakwaters. It is noted that the structure is effective for intercepting longshore sediment movement, not only for cross-shore movement. In Regions 3, shore-

line was rather stable except the left end, 0m<x<500m. The pre-tsunami shoreline behavior shows agreement with previous study's results (e.g., Kang and Tanaka, 2005).

It is seen in Figure 3 that after the tsunami, the rate of shoreline change has totally been modified. The rate of shoreline change is either almost zero or negative in Region 1 because of no supply of sediment from the right end (Mori et al., 2015). Slight recovery of shoreline has occurred in Regions 2, and serious retreat is observed in Region 3.
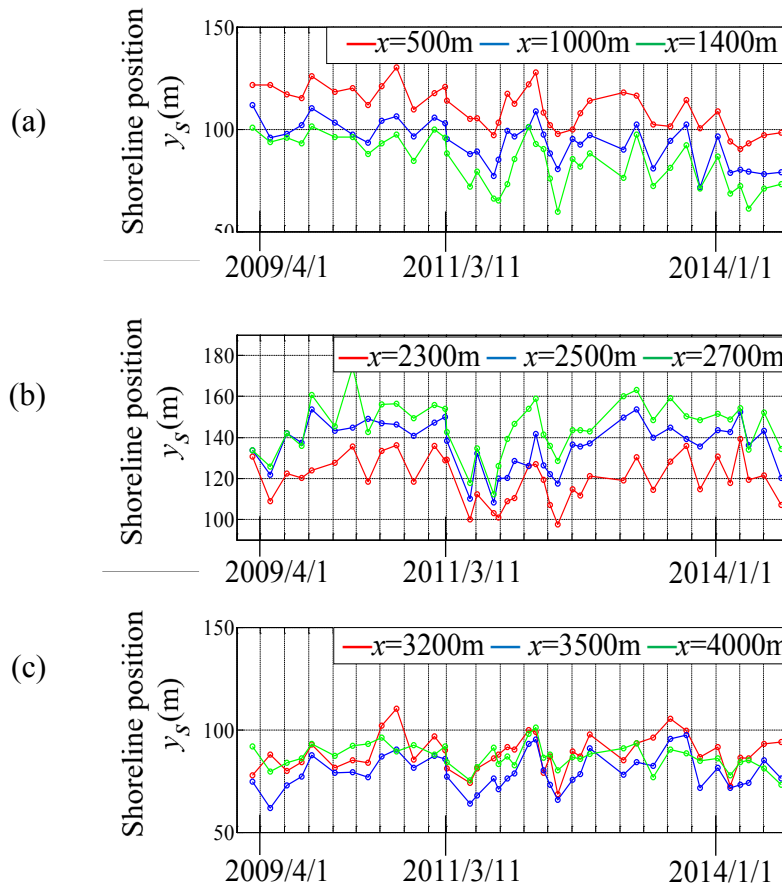
Figure 2. Shoreline change
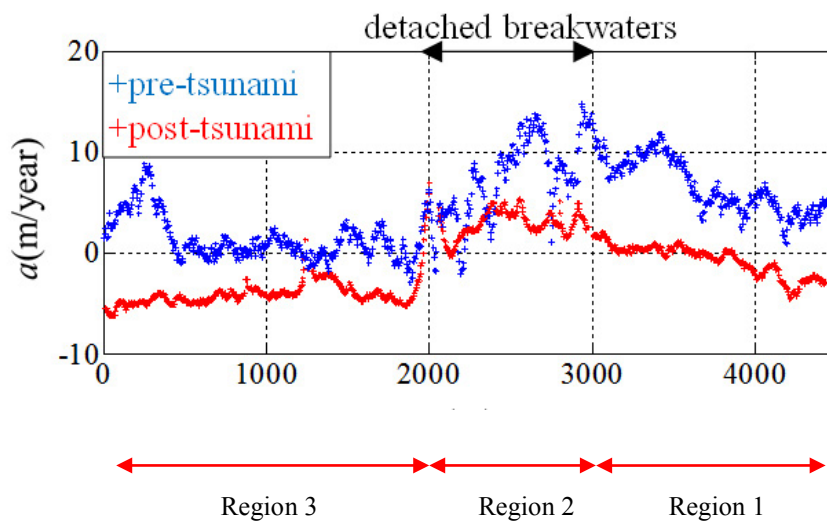
Figure 3. Rate of shoreline change.

3.2 EOF analysis for pre-tsunami period

The feature of shoreline change is extracted by using empirical orthogonal function (EOF) analysis separately for pre- and post-tsunami periods. EOF analysis has extensively been applied by many researchers to extract significant components of shoreline change (Winant et al., 1975, Miller and Dean, 2007a, 2007b). This analysis method enables us to separate the shoreline position $y_s(x,t)$ into spatial and temporal functions. In the present analysis, the difference from mean position is used for EOF analysis as defined in Eq. (3).

$$y^*(x,t)=y_s(x,t)\text{-}\bar{y}_s(x)=\sum_{n=1}^{k} c_n(t)e_n(x) \qquad (3)$$

where $\bar{y}_s(x)$ is the mean shoreline position, $y^*(x, t)$ is the shoreline position from the averaged one, $c_n(t)$ is the temporal eigenfunction, and $e_n(x)$ is the spatial eigenfuntion. Here the contribution of the n-th component is defined by

$$R_n=\lambda_n\Big/\sum_{i=1}^{k}\lambda_i \qquad (4)$$

Table 1 summarizes contribution of each component for pre- and post-tsunami periods. It is noted that the 1st and 2nd components are highly predominant as compared with the 3rd components. Hence detail results up to the 2nd component will be described hereafter.

Spatial and temporal functions during pre-tsunami period are plotted in Figures 4 and 5 for the 1st and 2nd components, respectively. In addition $y_n=e_n(x)c_n(t)$ is shown in Figures 6 and 7 for each component. It is noted that $e_1(x)$ is positive along the entire shoreline, indicating simultaneous retreat or advancement dependent on the sigh of the temporal function. Thus it can be concluded that the 1st component corresponds to shoreline change induced by cross-shore sediment movement. On the contrary to the 1st component, $e_2(x)$ function of the 2nd component depicted in Figure 5 shows opposite sign on the right and left hand sides of the offshore breakwaters. This corresponds to shoreline change induced by longshore sediment movement as already reported by Tanaka and Nagasawa (2002).

Table 1 Contribution of each component from EOF analysis

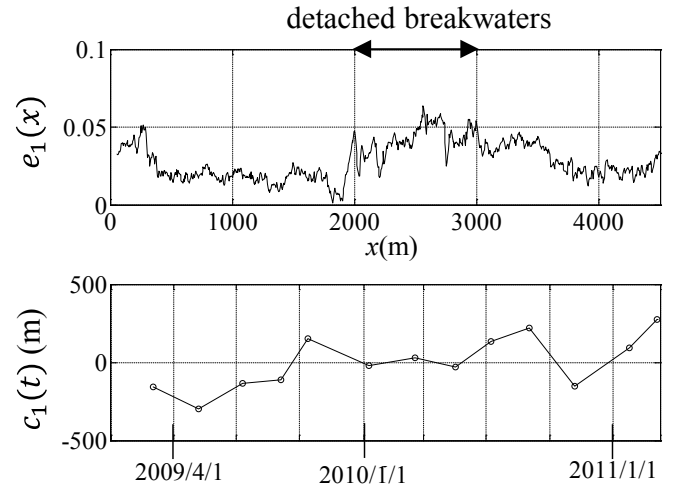|	1st Comp.	2nd Comp.	3rd Comp.
Pre-tsunami	50.0	21.2	7.7
Post-tsunami	57.4	21.5	5.8

Figure 4. $e_1(x)$ and $c_1(t)$ for pre-tsunami period
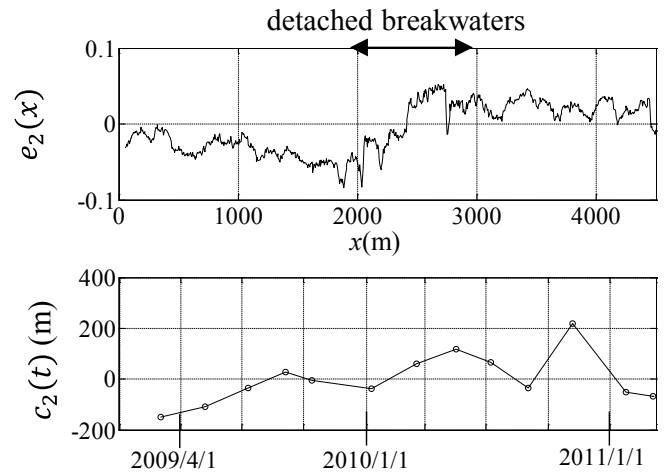

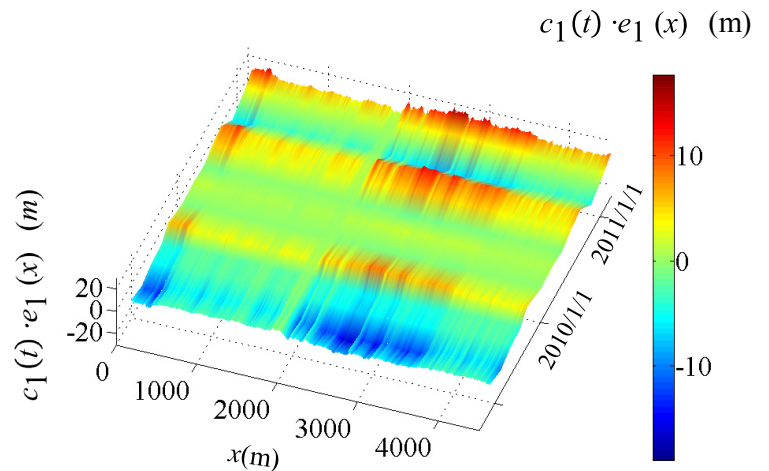Figure 5. $e_2(x)$ and $c_2(t)$ for pre-tsunami period

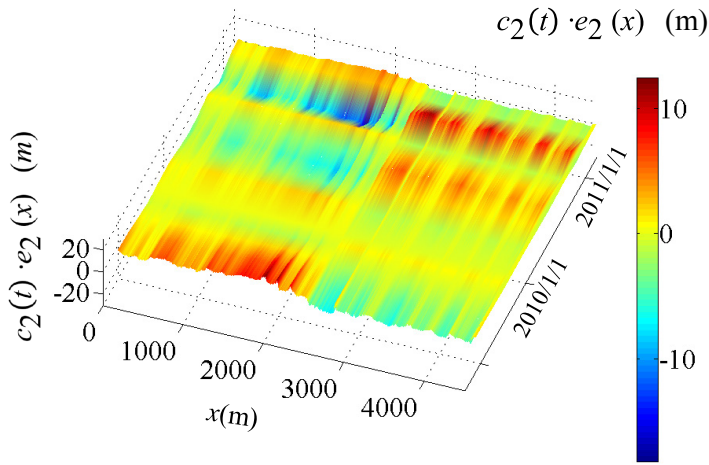Figure 6. Shoreline change due to the 1st component during pre-tsunami period

Figure 7. Shoreline change due to the 2nd component during pre-tsunami period
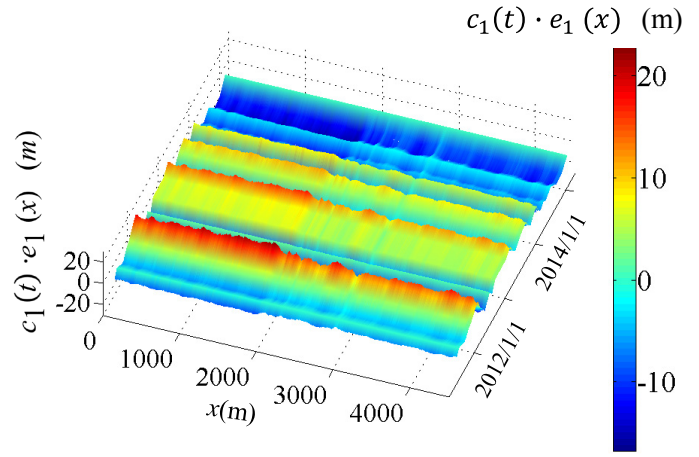

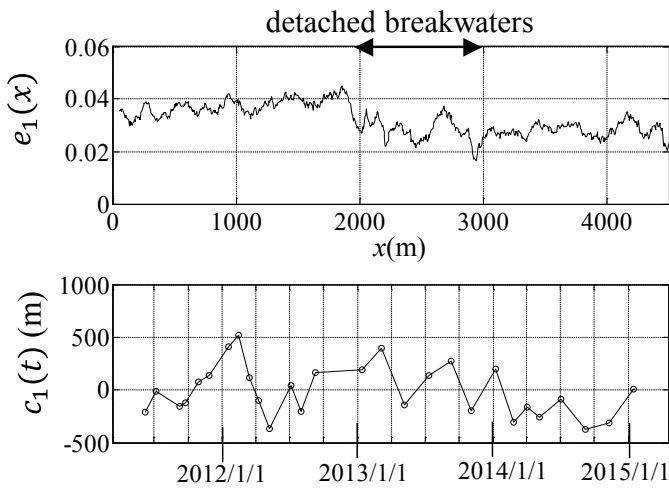Figure 10. Shoreline change due to the 1st component during post-tsunami period

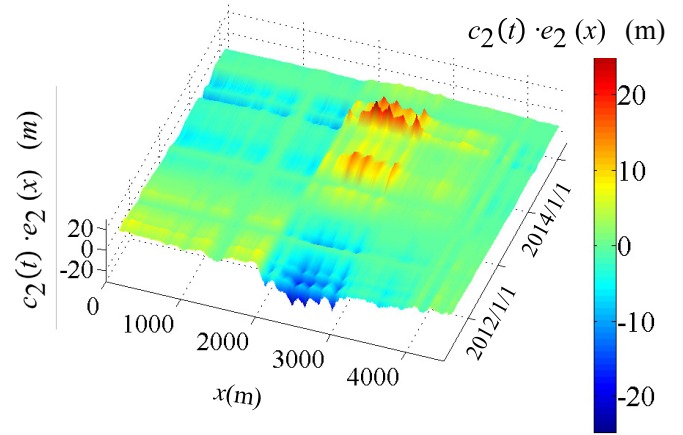Figure 8. $e_1(x)$ and $c_1(t)$ for post-tsunami period

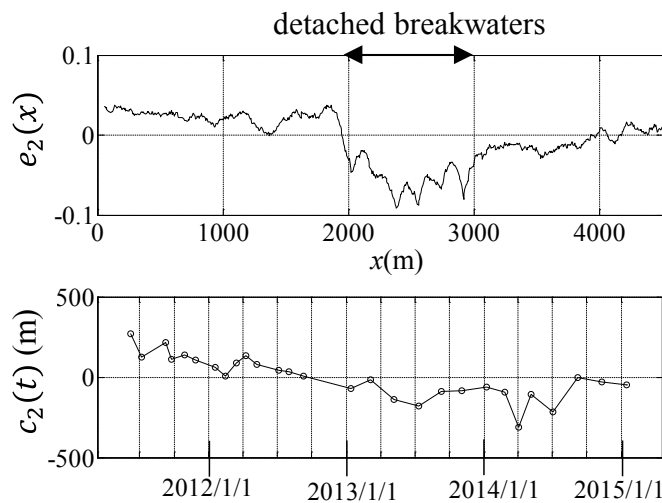Figure 11. Shoreline change due to the 2nd component during post-tsunami period

Figure 9. $e_2(x)$ and $c_2(t)$ for post-tsunami period

3.3 EOF analysis for post-tsunami period

Next, similar EOF analysis results for post-tsunami period are depicted in Figures 8, 9, 10 and 11. It is interesting to note that $e_1(x)$ in Figure 8 shows behavior highly similar to that shown in Figure 4 prior to the tsunami, indicating simultaneous shoreline retreat and advancement due to cross-shore sediment movement. Hence it is concluded that cross-shore shoreline change process is unchanged between pre- and post-tsunami periods.

Comparing pre- and post-tsunami $e_2(x)$ functions illustrated Figures 5 and 9, highly difference can be recognized, especially predominance of the negative value behind the offshore breakwater in Figure 9. Considering change in sign of $c_2(t)$ in Figure 9 from positive to negative in the recent years, the 2nd component mainly indicates sediment deposit behind the offshore breakwaters as clearly observed in Figure 11, whereas the shoreline change in Figure 10 shows

simultaneous shoreline change in the longshore direction. From Figures 9 and 11, it is observed that modification of the littoral system due to the 2011 Tsunami is successfully detected by the 2nd component of EOF analysis.

4 CONCLUSIONS

Shoreline change around offshore breakwaters located on Sendai Coast is investigated for pre- and post-tsunami periods through aerial photograph analysis. The followings are main conclusions drawn from the present study.

(1) Tombolo behind the breakwaters on Sendai Coast has totally been eroded by the 2011 Tsunami waves. After the erosion, tombolo has been re-formed, although the shoreline in the northern area shows distinct retreat.

(2) The 1st component from EOF analysis originates from cross-shore sediment movement, while the 2nd component corresponds to longshore sediment transport. The spatial function $e_1(x)$ for both pre- and post-tsunami does not show remarkable longshore variation, indicating simultaneous retreat or advancement independent on the longshore location.

(3) The 2nd component shows significant modification after the 2011 Tsunami, especially behind the offshore breakwaters. The shoreline position change expressed by the 2nd component mainly represents recovery process tombolo behind the offshore breakwaters. It seems that development of a new tombolo has been completed by now.

5 ACKNOWLEDGEMENT

REFERENCES

Hunt, I. A. 1959. Design of seawalls and breakwaters, *Journal of Waterway, Harbors Division, Am. Soc. Civ. Eng.*, 85(3), 123-152.

Kang, H.W. and Tanaka, H. 2005. Influence of cross-shore sediment movement on long-term shoreline change simulation, *Proceedings of 4th International Conference on River, Coastal and Estuarine Morphodynamics*, 343-348.

Miller, J.K., and R.G. Dean. 2007a. Shoreline variability via empirical orthogonal function analysis: Part I temporal and spatial characteristics, *Coastal Engineering*, 54(2), 111-131.

Miller, J.K., and R.G. Dean. 2007b. Shoreline variability via empirical orthogonal function analysis: Part II relationship to nearshore conditions, *Coastal Engineering*, 54(2), 133-150.

Mori, F., Mitobe, Y. and Tanaka, H. 2015. Littoral environment modification due to tsunami around detached breakwaters, *Journal of Jap. Soc. Civ. Eng. (Ocean Eng.)*, 71(2), I_647-I_652, 2015. (in Japanese)

Numata, A. and Takahashi, T. 1983. Shoreline change before and after offshore breakwater construction on Arahama Coast, Sendai, *Journal of Jap. Soc. Civ. Eng. (Coastal Eng.)*, 30, 269-273. (in Japanese)

Tanaka, H. and Nagasawa, T. 2002. Analysis of shoreline change on Sendai Coast using empirical eigen function method, *Proceedings of 13th APD-IAHR Congress*, 836-841.

Tanaka, H., Tinh, N.X., Umeda, M., Hirao, R., Pradjoko, E., Mano, A. and Udo, K. 2012. Coastal and estuarine morphology changes induced the 2011 Great East Japan Earthquake Tsunami, *Coastal Engineering Journal*, 54(1).

Udo, K., Sugawara, D., Tanaka, H., Imai, K. & Mano, A. 2012. Impact of the 2011 Tohoku earthquake and tsunami on beach morphology along the northern Sendai Coast, *Coastal Engineering Journal*, 54(1).

Winant, C.D., Inman, D.L. and Nordstrom, C.E. 1975. Description of seasonal beach changes using empirical eigenfunctions, *Journal of Geophysical Research*, 80(15), 1979-1986.